

# ADVANCED POLARIZATION AND ENERGY CONTROL FOR APPLE-II TYPE UNDULATOR BEAMLINES AT MAX-IV

Á. Freitas\*, B. Bertrand, M. Holz, M. Lindberg, J. Lidón-Simón, C. Takahashi, H. Tarawneh, L. Zhu  
MAX IV Laboratory, Lund University, Lund, Sweden

## Abstract

Precise control of photon beam properties is essential for modern synchrotron beamlines, particularly those utilizing APPLE-II type undulators. This paper presents the control system architecture developed at MAX-IV using IcePAP drivers and TANGO control system to achieve advanced polarization and energy manipulation. The system implements the BLUES (Beamline Universal Polarization Mode) framework, allowing dynamic control of both helical and inclined polarization states through synchronized phase motor settings. Central to this approach is the use of parametric lookup tables to define nonlinear motion trajectories for the undulator gap and phase axes. This system enables linear energy ramps, supporting constant electron volts per second (eV/s) scans crucial for high-resolution spectroscopy and imaging techniques, taking full advantage of the high flux provided by fourth-generation light sources and improving data collection efficiency without compromising the stability or quality of the photon beam. Integration between the beamline and accelerator control systems allows for the complex coordination required to manage polarization settings. To ensure electron beam stability during undulator motion, the control system integrates feedforward correction loops that compensate for orbit and optics distortions induced by gap and phase changes. This approach offers a scalable and precise method for enhancing beamline capabilities, tailored specifically for the challenges posed by APPLE-II undulators.

## INTRODUCTION

The MAX-IV Laboratory in Lund, Sweden, is the first diffraction-limited storage ring in the world. It is composed by two storage rings at 1.5 GeV and 3 GeV with a full energy injector (linac). The linac serves as both an injector for the storage rings and a driver for the Short Pulse Facility (SPF), enabling femtosecond-scale time-resolved experiments [1].

Soft X-ray beamlines at MAX-IV are primarily located on the 1.5 GeV ring and selected sections of the 3 GeV ring. These beamlines rely on APPLE-II type undulators, which are elliptically polarizing devices capable of producing variable polarization states linear (horizontal and vertical), circular, and elliptical by adjusting the relative phase of magnet arrays. This capability is essential for experiments requiring precise control over photon polarization, such as X-ray magnetic circular dichroism (XMCD), X-ray linear dichroism (XLD), resonant inelastic X-ray scattering (RIXS), X-ray absorption spectroscopy (XAS), and ambient-pressure photoelectron spectroscopy (APXPS). Polarization control is a

\* aureo.freitas@maxiv.lu.se

fundamental requirement in synchrotron-based soft X-ray spectroscopy. The polarization state of the incident photons—linear, circular, or elliptical—directly influences the interaction mechanisms between X-rays and matter, thereby determining the sensitivity and specificity of various spectroscopic techniques. Figure 1 illustrates the polarizations schema.

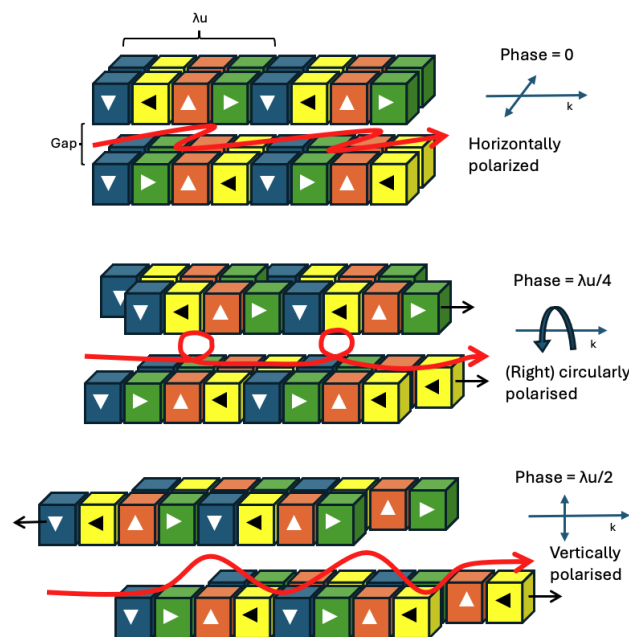


Figure 1: Polarization schema example of APPLE-II.

Currently, MAX-IV operates several APPLE-II undulators built in-house [2], including those that serve the HIPPIE, Veritas, and SoftiMAX beamlines on the 3 GeV ring. These devices offer high brilliance and polarization flexibility across the soft X-ray spectrum. Additionally, the BLOCH beamline on the 1.5 GeV ring utilizes a quasi-APPLE-II undulator, extending the facility's polarization control capabilities at lower photon energies.

## MAX-IV APPLE-II CONTROL SYSTEM

The MAX-IV APPLE-II undulator is driven by eight independent servomotors:  $x_1, x_2, x_3, x_4$  control the longitudinal phase (phase motors), and  $z_1, z_2, z_3, z_4$  control the magnetic gap. The system uses IcePAP [3] controllers to interface with the servo drives, allowing the servomotors to be controlled in a stepper-like fashion. Position feedback is provided by absolute encoders, enabling closed-loop control via an integral controller. Additional PLC-connected encoders are

installed for the Machine Protection System (MPS) and Personnel Protection System (PSS); these interlock signals can inhibit or stop IcePAP motion when safety conditions are not met. The MAX-IV PLC platform is based on Rockwell Allen-Bradley hardware. Accelerator operators can use Tango Locker functionality to inhibit undulator control from beamlines.

The facility control system is based on Tango [4], which integrates both the PLC and IcePAP controllers. The application layer is implemented in Python. Sardana [5] is used to expose each axis as a motor, with all configuration parameters published as Tango attributes. The PLC Tango interface exposes all relevant tags and alarms for machine protection. Sardana pseudo-motors are used to create high-level composite motors representing physical quantities such as *gap*, *taper*, *offset*, as well as the individual phase motions: *helical* and *inclined*.

An additional Tango attribute defines the undulator mode, which determines how the phase motors are coordinated. MAX-IV supports six basic modes: Modes 1–3 correspond to helical configurations, and Modes 4–6 correspond to inclined configurations. Furthermore, Universal Modes 7-10 are available [6], allowing simultaneous combination of helical and inclined components to produce arbitrary polarization states. Figure 2 illustrates the modes, motors and coordination.

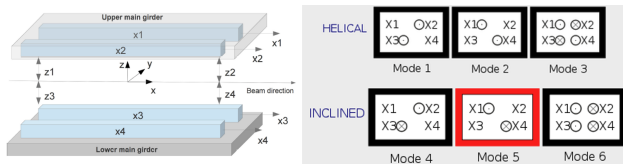


Figure 2: APPLE-II modes examples, motors and coordination.

All these components are located at Accelerator Control System. Figure 3 illustrates the Control System Schema. The subsections below describe the subsystems in detail.

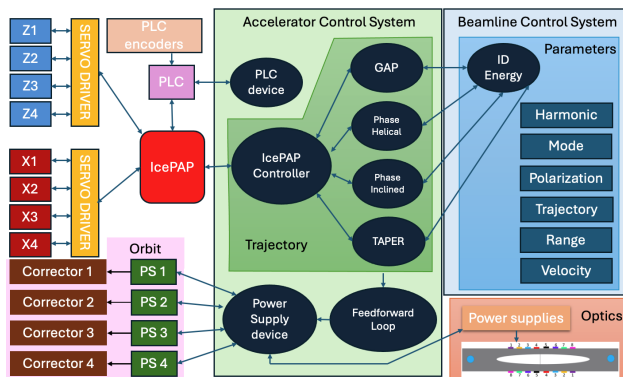


Figure 3: Control system schematics.

## Gap Calculation

The pseudo-parameters *gap*, *offset*, and *taper* are calculated from four input values  $z_1, z_2, z_3, z_4$  according to the following equations:

$$\text{gap} = \frac{1}{2} (z_1 + z_2 + z_3 + z_4) \quad (1)$$

$$\text{offset} = \frac{1}{4} (z_1 - z_3 + z_2 - z_4) \quad (2)$$

$$\text{taper} = (z_2 - z_1) + (z_4 - z_3) \quad (3)$$

Here:

- **gap** represents the average vertical position of the four  $z$  values, corresponding to the overall opening of the system.
- **offset** quantifies the vertical asymmetry between the upper and lower pairs, indicating a vertical shift of the magnetic structure with respect to the beam axis.
- **taper** represents the longitudinal difference between the upstream and downstream ends, describing a gradual change in gap along the device.

*Physical Interpretation* Physically, these parameters provide a compact description of the mechanical state of a variable-gap insertion device (such as an APPLE-II undulator). The *gap* controls the photon energy, the *offset* can be used to correct orbit distortions or apply vertical fields, and the *taper* enables fine adjustment of the field amplitude along the device to optimize lasing or compensate for beam energy spread.

## Phase Calculation

The phase control of an APPLE-II undulator is implemented by moving four longitudinal actuators ( $x_1, x_2, x_3, x_4$ ). Depending on the selected *mode*, the motion pattern of these actuators produces different polarization states of the emitted light.

Let  $o$  be the desired phase offset. The actuator positions  $x_1, x_2, x_3, x_4$  are assigned according to:

### Helical Modes

#### • Mode 1:

$$x_2 = x_3 = o, \quad x_1, x_4 \text{ fixed}$$

Produces a helical trajectory where  $x_2$  and  $x_3$  move in parallel while  $x_1$  and  $x_4$  remain fixed.

#### • Mode 2:

$$x_1 = x_4 = o, \quad x_2, x_3 \text{ fixed}$$

Produces a helical trajectory with  $x_1$  and  $x_4$  moving in parallel and  $x_2, x_3$  fixed.

- **Mode 3:**

$$x_1 = x_4 = \frac{o}{2}, \quad x_2 = x_3 = -\frac{o}{2}$$

Produces a symmetric helical mode with all actuators moving, resulting in a centered phase shift.

### Inclined Modes

- **Mode 4:**

$$x_2 = o, \quad x_3 = -o, \quad x_1, x_4 \text{ fixed}$$

Produces linear polarization inclined with respect to the horizontal axis by moving  $x_2$  and  $x_3$  in opposite directions.

- **Mode 5:**

$$x_1 = o, \quad x_4 = -o, \quad x_2, x_3 \text{ fixed}$$

Produces linear polarization inclined with respect to the vertical axis by moving  $x_1$  and  $x_4$  in opposite directions.

- **Mode 6:**

$$x_1 = \frac{o}{2}, \quad x_2 = -\frac{o}{2}, \quad x_3 = \frac{o}{2}, \quad x_4 = -\frac{o}{2}$$

Produces a diagonal inclined mode by moving all actuators in an antiparallel pattern.

*Universal Modes* In *universal mode*, two independent parameters are used: a *helical offset*  $h$  and an *inclined offset*  $i$ , allowing the generation of arbitrary polarization states.

- **Mode 7:**

$$x_1 = h, \quad x_2 = i, \quad x_3 = -i, \quad x_4 = h$$

Combines parallel motion of  $x_1$  and  $x_4$  (helical contribution) with antiparallel motion of  $x_2$  and  $x_3$  (inclined contribution).

- **Mode 8:**

$$x_1 = i, \quad x_2 = h, \quad x_3 = h, \quad x_4 = -i$$

Combines antiparallel motion of  $x_1$  and  $x_4$  with parallel motion of  $x_2$  and  $x_3$ .

- **Mode 9:**

$$x_1 = h, \quad x_2 = i, \quad x_3 = -i, \quad x_4 = h$$

Equivalent to Mode 7 but with a different motion envelope (e.g. for safety or mechanical constraints).

- **Mode 10:**

$$x_1 = i, \quad x_2 = h, \quad x_3 = h, \quad x_4 = -i$$

Equivalent to Mode 8 but with a different motion envelope.

*Physical Interpretation* These motion patterns correspond to the relative longitudinal displacements of the four magnet arrays in an APPLE-II undulator. The *helical modes* (1–3) generate left- or right-handed circular polarization depending on the sign of  $o$ , while the *inclined modes* (4–6) generate linearly polarized light rotated with respect to the horizontal plane. The *universal modes* (7–10) allow independent control of the helical and inclined components, enabling the generation of arbitrary polarization states (including elliptical polarization) in a continuous and reproducible way.

### Correction

All pseudo-positions are continuously streamed to a dedicated Tango device that implements a feedforward control loop running at 10 Hz. This device uses look-up tables that monitor *gap*, *taper*, *offset*, and *phase* positions in order to apply real-time corrections to both orbit and optics [7].

Orbit correction is performed using horizontal and vertical corrector magnets mounted on either side of the undulator girder. For optics correction, eight printed copper strips are installed on the vacuum chamber to compensate for the quadrupole field components generated by the undulator's field.

The feedforward device is designed to accept an arbitrary number of inputs ( $n$ ) and generate an arbitrary number of outputs ( $m$ ). It computes the necessary corrections and writes the corresponding setpoints to the power-supply Tango devices, which in turn deliver the required currents to the magnets.

At the moment, a solution for ID correction using machine learning strategies is being tested at MAX IV [8], with the work motivated by the challenges posed by more complex undulators such as the Apple-II. This approach aims to improve the characterization of the feature and actuator spaces, potentially offering more adaptive correction, better generalization across operational conditions, and reduced maintenance efforts compared to traditional empirically derived look-up tables.

### Undulator Energy

The undulator energy controls are implemented at each Beamline Control System and operate on top of the pseudo-parameters (*gap*, *offset*, *taper*, and *phase*). The energy setpoint is calculated using either look-up tables derived from undulator field maps or a higher-order polynomial fit, depending on the precision required. These controls allow for direct manipulation of both harmonic content and polarization state of the emitted radiation. Calibration of the energy control is performed using a polarimeter, and the resulting corrections are applied individually for each beamline branch to ensure accurate photon energy delivery and polarization purity.

In addition, the system supports non-linear parametric trajectories, which enables continuous energy scans at a constant rate in electron volts per second (eV/s). This capability is particularly important for experiments requiring

smooth and precise energy sweeps, minimizing mechanical vibrations or field deviations, and allowing seamless synchronization with other beamline components such as monochromators and detectors [9].

## CONCLUSION

Since the first beam at MAX-IV, this system has been successfully implemented and is now in operation at seven beamlines. Its performance over several years demonstrates that it is both robust and reliable, providing a flexible and precise platform for photon beam control across multiple experimental stations. Figure 4 illustrates the Iron  $L_{2,3}$ -edge X-Ray Absorption (XAS) spectra at HIPPIE beamline for circular right and left polarization.

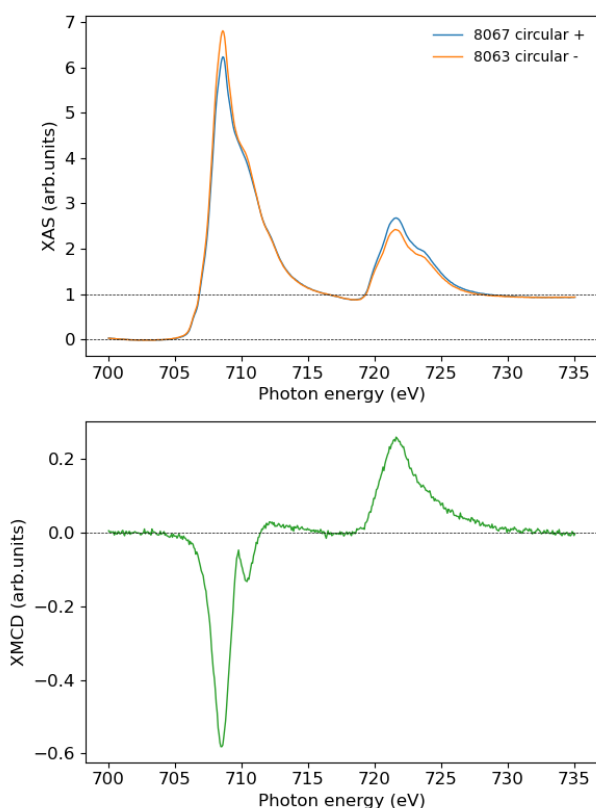


Figure 4: Iron  $L_{2,3}$ -edge X-Ray Absorption (XAS) spectra at HIPPIE beamline for circular polarization.

## FUTURE DEVELOPMENT

Plan to integrate the same Control System and functionalities for the in-house developed APPLE-X [10] at possible MAX-IV SXL FEL [11] and 3 GeV ring.

## ACKNOWLEDGMENTS

The authors acknowledge the support of the MAX-IV Software Group, the Accelerator Development Group and the Soft X-ray Beamline staff for their assistance and contribution to this work.

## REFERENCES

- [1] N. Martensson and M. Eriksson, “The saga of MAX IV, the first multi-bend achromat synchrotron light source”, *Nucl. Instrum. Methods Phys. Res., Sect. A*, vol. 907, pp. 97–104, Nov. 2018. doi:10.1016/j.nima.2018.03.018
- [2] H. Tarawneh, A. Thiel, and M. Ebbeni, “First commissioning results of phase I insertion devices at MAX IV Laboratory”, *Proc. AIP Conf.*, vol. 2054, p. 030023, 2019. doi:10.1063/1.5084586
- [3] N. Janvier *et al.*, “IcePAP: An Advanced Motor Controller for Scientific Applications in Large User Facilities”, in *Proc. ICALEPCS'13*, San Francisco, CA, USA, Oct. 2013, paper TUPPC081, pp. 766–769.
- [4] A. Gotz *et al.*, “The TANGO Controls Collaboration in 2015”, in *Proc. ICALEPCS'15*, Melbourne, Australia, Oct. 2015, pp. 585–588. doi:10.18429/JACoW-ICALEPCS2015-WEA3001
- [5] T. M. Coutinho *et al.*, “Sardana: The Software for Building SCADAS in Scientific Environments”, in *Proc. ICALEPCS'11*, Grenoble, France, Oct. 2011, paper WEAUST01, pp. 607–609.
- [6] H. Tarawneh *et al.*, “Universal mode of operation of the APPLE II undulators at the MAX IV 1.5 GeV ring”, presented at the IPAC'25, Taipei, Taiwan, Jun. 2025, paper TUPM066, unpublished.
- [7] C. Takahashi *et al.*, “Multi-Dimensional Feedforward Controller at MAX IV”, in *Proc. IBIC'22*, Kraków, Poland, Sep. 2022, pp. 335–338. doi:10.18429/JACoW-IBIC2022-TUP41
- [8] C. Takahashi *et al.*, “Multi-Dimensional Feedforward Controller at MAX IV”, in *Proc. IBIC'22*, Kraków, Poland, Sep. 2022, pp. 335–338. doi:10.18429/JACoW-IBIC2022-TUP41
- [9] Á. Freitas *et al.*, “Position-based continuous energy scan status at MAX IV”, in *Proc. ICALEPCS'23*, Cape Town, South Africa, Oct. 2023, pp. 917–920. doi:10.18429/JACoW-ICALEPCS2023-TUPDP145
- [10] H. Tarawneh, M. Holz, and L. Roslund, “Full-scale compact APPLE X prototype undulator at MAX IV - characterization and measurements results”, *Nucl. Instrum. Methods Phys. Res., Sect. A*, vol. 1072, p. 170162, Mar. 2025. doi:10.1016/j.nima.2024.170162
- [11] S. Werin *et al.*, “The Soft X-Ray Laser Project at MAX IV”, in *Proc. IPAC'17*, Copenhagen, Denmark, May 2017, pp. 2760–2762. doi:10.18429/JACoW-IPAC2017-WEPAB077